Effects of Magnetic Shear on Toroidal Rotation in Tokamak Plasmas with Lower Hybrid Current Drive

J. E. Rice, Y. A. Podpaly, M. L. Reinke et al

Effects of Magnetic Shear on Toroidal Rotation in Tokamak Plasmas
with Lower Hybrid Current Drive

J. E. Rice,[1] Y. A. Podpaly,[1] M. L. Reinke,[1] R. Mumgaard,[1] S. D. Scott,[2] S. Shiraiwa,[1] G. M. Wallace,[1] B. Chouli,[3]
C. Fenzi-Bonizec,[3] M. F. F. Nave,[4] P. H. Diamond,[5] C. Gao,[1] R. S. Granetz,[1] J. W. Hughes,[1] R. R. Parker,[1] P. T. Bonoli,[1]
L. Delgado-Aparicio,[2] L.-G. Eriksson,[6] C. Giroud,[7] M. J. Greenwald,[1] A. E. Hubbard,[1] I. H. Hutchinson,[1] J. H. Irby,[1]
K. Kirov,[7] J. Mailloux,[7] E. S. Marmar,[1] and S. M. Wolfe[1]

[1]*PSFC MIT, Cambridge, Massachusetts 02139, USA*
[2]*PPPL, Princeton, New Jersey 08543, USA*
[3]*CEA-Cadarache, 13108 St.-Paul-lez-Durance, France*
[4]*Associação EURATOM/IST, Universidade Técnica de Lisboa, 1049-001, Lisbon, Portugal*
[5]*CMTFO, UCSD, San Diego, California 92903, USA*
[6]*European Commission, Research Directorate General, B-1049 Brussels, Belgium*
[7]*CCFE/Euratom Fusion Association, Abingdon OX14 3DB, United Kingdom*
(Received 24 May 2013; published 17 September 2013)

Application of lower hybrid (LH) current drive in tokamak plasmas can induce both co- and counter-current directed changes in toroidal rotation, depending on the core q profile. For discharges with $q_0 < 1$, rotation increments in the countercurrent direction are observed. If the LH-driven current is sufficient to suppress sawteeth and increase q_0 above unity, the core toroidal rotation change is in the cocurrent direction. This change in sign of the rotation increment is consistent with a change in sign of the residual stress (the divergence of which constitutes an intrinsic torque that drives the flow) through its dependence on magnetic shear.

The benefits of rotation and flow shear for tokamak performance are well known. Rotation can suppress dele-terious MHD modes whereas velocity shear can break up turbulent eddies leading to an improvement in confine-ment. Toroidal rotation is often driven externally through neutral beam injection, but beam torque is expected to be small in future fusion devices, so other methods for rota-tion drive are necessary. One possibility is to take advan-tage of self-generated flow in enhanced confinement regimes [1], but this process relies on plasma performance, which makes for a complicated control knob. Another approach is to utilize radio frequency waves (ion cyclotron, electron cyclotron, and lower hybrid), although the mecha-nisms of direct generation of rotation are not well under-stood. Ion cyclotron range of frequencies mode conversion flow drive has been demonstrated [2], and rotation effects from electron cyclotron heating have been seen [3]. Toroidal rotation changes due to lower hybrid (LH) waves have also been observed [4–10], with velocities in both the co- and countercurrent directions. Even in plasmas with good core absorption of LH waves, the mechanism for rotation drive is not clear. Candidates include direct mo-mentum input from the waves (calculated to be low [7]), electron orbit loss [4], trapped electron pinch effects [11], resonant electron radial drift [12,13], and less direct causes such as the turbulent equipartition pinch [8] or through modification of the q profile [9,10]. A challenge of these accounts is to explain the rotation changes observed in both directions. To this end, this Letter compares the response

of rotation to the q profile in Alcator C-Mod, Tore Supra, and JET LH current drive (LHCD) plasmas.

Shown in Fig. 1 is a comparison of core toroidal rotation velocity time histories for two discharges with LHCD (~ 0.8 MW, with parallel index of refraction $n_\parallel = 1.6$) at line averaged densities of $\langle n_e \rangle = 0.7 \times 10^{20}/\mathrm{m}^3$ and magnetic fields of 5.4 T from Alcator C-Mod ($R = 0.67$ m, $a \sim 0.21$ m), with plasma currents of 0.91 MA ($q_{95} = 3.7$) and 0.42 MA ($q_{95} = 7.7$). For the higher current case, there was change in core rotation (from the initial $+20$ km/s) in the countercurrent direction of ~ 30 km/s, which evolved on a current relaxation time scale (100s of ms), considerably longer than the momentum confinement time (10s of ms). For the lower current case, there was an increment of ~ 30 km/s in the cocurrent direction, from an initial velocity of about -50 km/s. The 0.91 MA discharge had sawtooth oscillations throughout the duration of the lower-hybrid range of frequencies wave injection, whereas the sawteeth in the 0.42 MA plasma were stabilized beginning at 0.97 s.

Velocity profiles in C-Mod determined from x-ray imaging spectroscopy [14] for high and low plasma current discharges with $\langle n_e \rangle = 0.7 \times 10^{20}/\mathrm{m}^3$, before and during injection of ~ 0.8 MW of LHCD power, are shown in Fig. 2. For the 0.71 MA Ohmic target plasma, the profile is relatively flat, with a cocurrent velocity around $+20$ km/s across the profile. For the 0.42 MA Ohmic target plasma, the profile is strongly countercurrent in the core and has a steep gradient region just inside of the
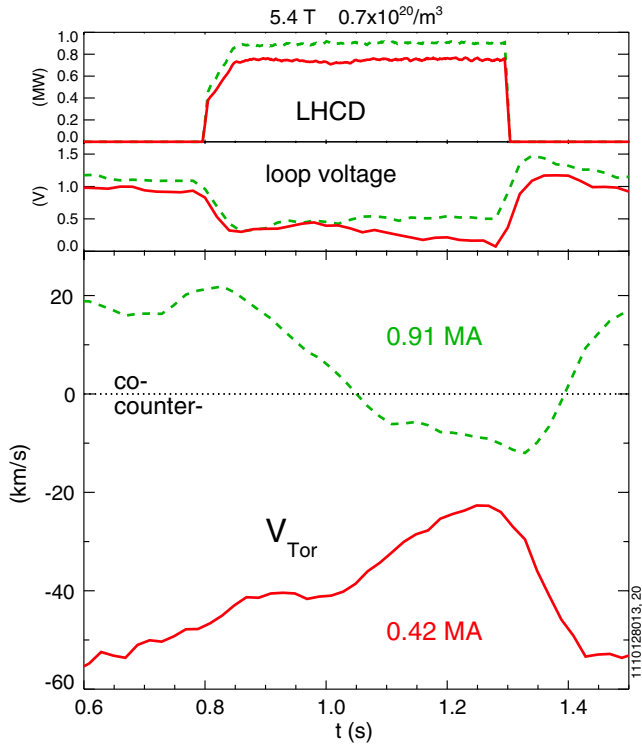
FIG. 1 (color online). Time histories of the LHCD power, loop voltage, and core toroidal rotation velocity for 5.4 T discharges from Alcator C-Mod, with plasma currents of 0.91 MA (green dashed line) and 0.42 MA (solid red line).

midradius. The profiles are similar during the LHCD, becoming slightly countercurrent in the core. The particular shape evolution of the high current discharge, which changes sign in the core region, suggests that these profiles are not the result of a momentum pinch effect, which could only alter the profile shape but not reverse the direction. There is no change in the profiles outside of the midradius
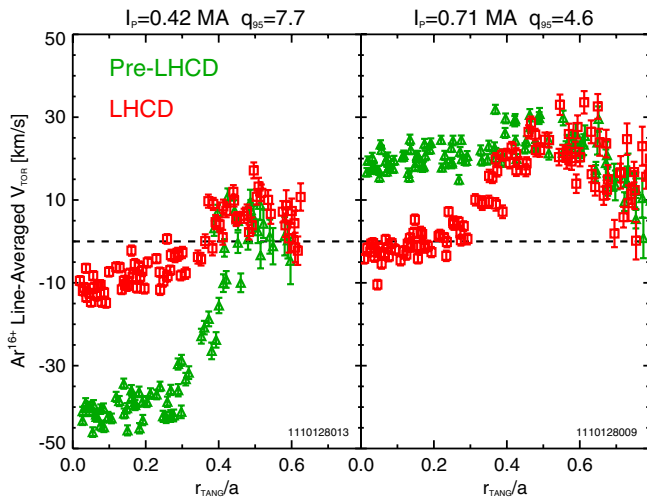

FIG. 2 (color online). Toroidal rotation spatial profiles before (green triangles) and during (red squares) LHCD for 0.42 MA (left) and 0.71 MA (right) C-Mod discharges.

($r/a \sim 0.5$) with LHCD [5,6]. Similar rotation profile behavior has been seen in JET [7,10] and Tore Supra LHCD plasmas. This anchoring of the profiles in the vicinity of the midradius is reminiscent of what is observed during Ohmic rotation reversal [15].

It is a challenge to understand what causes these bidirectional rotation changes with LHCD. This observed bidirectionality seems to rule out direct momentum input, since the waves are launched in the same direction in both cases. The input torque from LH waves [7,12], $Rn_{\parallel}P_{LH}/c \sim 0.002$ N m (for the cases shown in Fig. 1), is directed countercurrent. To address this rotation increment direction issue, an examination of rotation characteristics has been performed during a dedicated shot-by-shot plasma current scan.

The change or increment in the core rotation velocity in C-Mod (the difference in the time averaged velocity at the end of the LHCD pulse, 1.2–1.3 s, and the pre-LHCD phase, 0.7–0.8 s) as a function of plasma current, for a series of similar 5.4 T C-Mod discharges with $n_e = 0.7 \times 10^{20}/m^3$ and LHCD power between 0.75 and 0.9 MW, is shown in the bottom panel of Fig. 3. The *change* in steady-state rotation with LHCD varies strongly with plasma current, going from $\sim +30$ km/s at the lowest current (0.32 MA, $q95 = 9.6$) to around -30 km/s at the highest current (0.91 MA, $q_{95} = 3.7$). There is a stagnation point for $I_P \sim 0.6$ MA ($q_{95} = 5.5$) for these particular target plasma conditions, where application of 0.8 MW of LHCD power has little effect on the central rotation. The
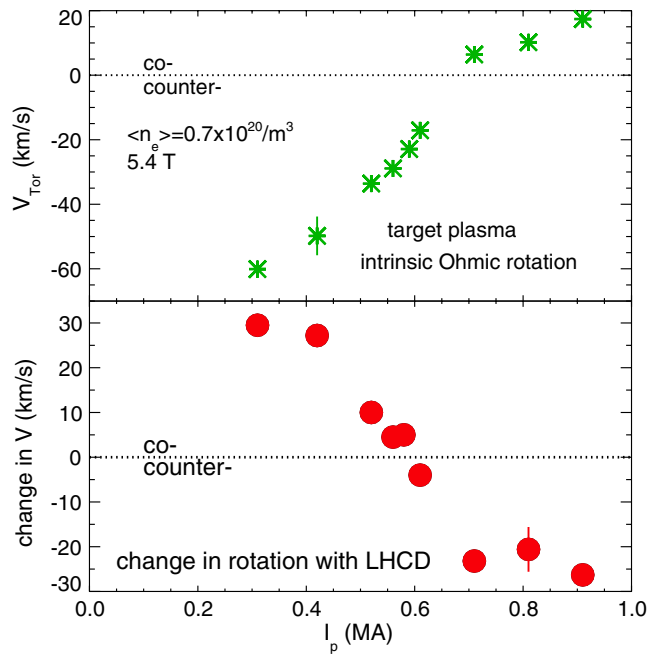

FIG. 3 (color online). The core toroidal rotation velocity as a function plasma current for 5.4 T C-Mod discharges with $n_e = 0.7 \times 10^{20}/m^3$, during the Ohmic phase before LHCD (top). The change in the central toroidal rotation velocity during LHCD as a function of plasma current (bottom).

TABLE I. Number of discharges, showing the correlation between sawteeth and rotation increment direction with LHCD, for low-density L-mode target plasmas from C-Mod.

	Sawteeth	No sawteeth
Corotation	0	89
Counterrotation	146	8

Ohmic heating power before LHCD for these discharges ranged from 0.39 MW at 0.32 MA to 1.04 MW at 0.91 MA. The zero crossing point for these discharges is very close to the intrinsic rotation reversal critical density and current [15–17], suggesting a possible connection between this bidirectional rotation change with LHCD and intrinsic Ohmic rotation reversals. As shown in the top panel of Fig. 3, the intrinsic rotation velocity of the Ohmic (pre-LHCD) target plasma also depends strongly on the plasma current [10,17] in this current scan. The core toroidal rotation varies from -60 km/s at the lowest I_P value to $+20$ km/s at the highest value, and this intrinsic Ohmic rotation switches direction at ~ 0.7 MA for this electron density and magnetic field, an example of the rotation reversal phenomenon [15–18]. The rotation profile anchoring shown in Fig. 2 and the similarity between the LHCD rotation bidirectionality and intrinsic Ohmic rotation reversal critical points suggest that the two phenomena may be related.

The cause of the flip in rotation direction for Ohmic plasmas is thought to be due to a reversal in sign of the residual stress [19] Π_r due to a change of domination from trapped electron modes to ion temperature gradient (ITG) modes above a critical collisionality (ν_*) [15–17]. Π_r is the component of the momentum flux not proportional to the velocity or its gradient, whose sign depends on the underlying turbulent modes. The divergence of Π_r is the intrinsic torque density. Π_r is also a function of the gradient of the current density profile [19–23] and, in principle, can switch sign through changes in the current density profile by externally driven current via LH waves.

Evidence for the role of the current density profile is suggested by changes in sawtooth behavior. LHCD plasmas that had sawtooth oscillations showed countercurrent velocity increments, whereas in the cocurrent rotation increment discharges, the sawteeth were suppressed due to a significant change in the q profile. Table I summarizes the sawtooth behavior for a database of 243 low density target C-Mod plasmas with LHCD. No coincrement discharges exhibited sawtooth oscillations whereas all sawtoothing discharges underwent countercurrent rotation changes. Only a few counterincrement plasmas were without sawteeth. LHCD discharges without sawteeth also experienced cocurrent rotation increments in JT-60U [4], EAST [8], JET [10], and Tore Supra. A summary of the LHCD rotation parameters from various tokamaks is shown in Table II. The first column gives the rotation increment direction following LHCD.

Current density profiles for C-Mod plasmas have been determined from magnetics calculations constrained by motional Stark effect observations [24,25] enabled by a diagnostic neutral beam. The inverse rotational transform q, magnetic shear ($\hat{s} = r/q \partial q/\partial r$), and magnetic shear scale length ($L_s \equiv R_0 q/\hat{s}$) profiles, for three discharges from Fig. 3 with plasma currents of 0.32, 0.58, and 0.91 MA, evaluated between 1.14 and 1.24 s, are shown in Fig. 4. For the 0.91 MA plasma (which was sawtoothing throughout the LHCD pulse), the q profile (top frame) increases monotonically, with q_0 well below 1 at the magnetic axis. The zero crossing at 0.75 m is consistent with the measured sawtooth inversion radius. For the 0.32 MA case, the q profile is flat in the core, with a value just under 2; for the 0.58 MA plasma, $q_0 \sim 1.3$. This is consistent with the lack of sawtooth oscillations for these latter two discharges. Another difference between these cases is the magnetic shear (middle frame); for the 0.91 MA plasma, $\hat{s}$ at $r/a \sim 0.3$ was about 0.5, for the 0.58 MA case, the core $\hat{s}$ was near 0.2, and for the 0.32 MA discharge, $\hat{s}$ in the core was close to 0. Interestingly, all three $\hat{s}$ profiles converge near the mid-radius, which is close to the rotation profile stagnation point shown in Fig. 2. For the 0.91 MA plasma, the magnetic shear scale length L_s (bottom frame) at $R = 0.75$ m ($r/a \sim 0.3$) was ~ 1.5 m whereas for the 0.58 MA

TABLE II. Machine and operational parameters for LHCD experiments in L-mode plasmas on various devices. The column identified as ΔV indicates the rotation increment direction relative to the plasma current. The column marked Sawtooth indicates whether or not there were sawtooth oscillations.

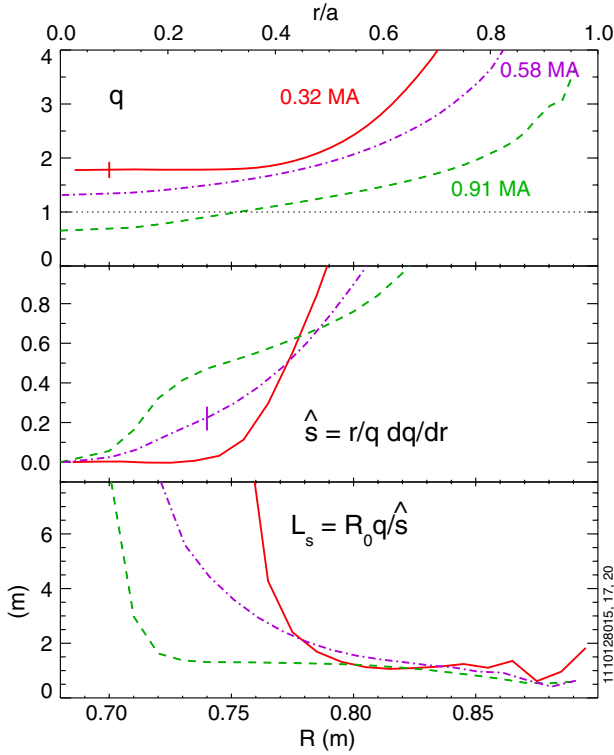| Device	ΔV	$n_e (10^{20}/m^3)$	q_{95}	Sawtooth	I (MA)	B (T)	R (m)	Reference
C-Mod	counter	0.6–1.2	<5	y	0.8	5.4	0.67	[5,6,9]
C-Mod	co	0.4–0.6	6–10	n	<0.6	5.4	0.67	[9]
EAST	co	0.08	10	n	0.25	2	1.8	[8]
JET	co	0.20	4.4	n	2	2.8	2.96	[7,10]
JET	counter	0.21	4.1	y	2	2.5	2.96	[10]
JT-60U	co	0.04	6.2	n	1.2	3.6	3.4	[4]
Tore Supra	co	0.47	3.9	n	0.7	2.2	2.34	
Tore Supra	counter	0.58	3.9	y	1.2	3.9	2.34	

FIG. 4 (color online).   The inverse rotational transform q (top), magnetic shear $\hat{s}$ (middle), and magnetic shear scale length L_s (bottom) profiles for 0.32 MA (red solid line), 0.58 MA (purple dash-dotted line), and 0.91 MA (green dashed line) C-Mod discharges with LHCD (1.14–1.24 s). Typical error bars are shown.

discharge was ~ 3 m. For the low current case, the core $\hat{s}$ hovers ~ 0, which gives rise to large values of L_s; $L_s \sim 20$ m at $R = 0.75$ m for the 0.32 MA plasma.

The connection between the core magnetic shear scale length and direction of rotation increment is illustrated in Fig. 5 where the change in the core rotation velocity with LHCD (1.14–1.24 s) is shown as a function of the average value of L_s near $r/a \sim 0.3$ for C-Mod discharges. There is an abrupt change in the LHCD rotation increment, going from counter- to co-, near $L_s \sim 2.3$ m, exhibiting a threshold behavior. The point for the cocurrent change 0.32 MA discharge with $L_s \sim 20$ m is off scale. Typical error bars are shown. A related threshold is seen as a function of the central inverse rotational transform, as is illustrated in Fig. 6, where the change in core rotation frequency is shown depending on q_0. The null in $\Delta \omega$ is close to $q_0 \sim 1$. The use of the rotation frequency allows for direct comparison with the results from other devices; also shown in Fig. 6 are points from EAST [8], JET [10], and Tore Supra, which fit well with those from C-Mod. These points generally occupy two quadrants in this operational space: countercurrent rotation increments for plasmas with $q_0 < 1$ and cocurrent for $q_0 > 1$. The change in rotation direction near $q_0 \sim 1$ appears to be independent of electron density, both from a comparison of these results from different devices and from dedicated experiments at C-Mod.

These changes in the q profiles are significant, because the structure of the residual stress Π_r [20–22] (which gives rise to an intrinsic torque via $\nabla \cdot \Pi_r$) and the turbulent
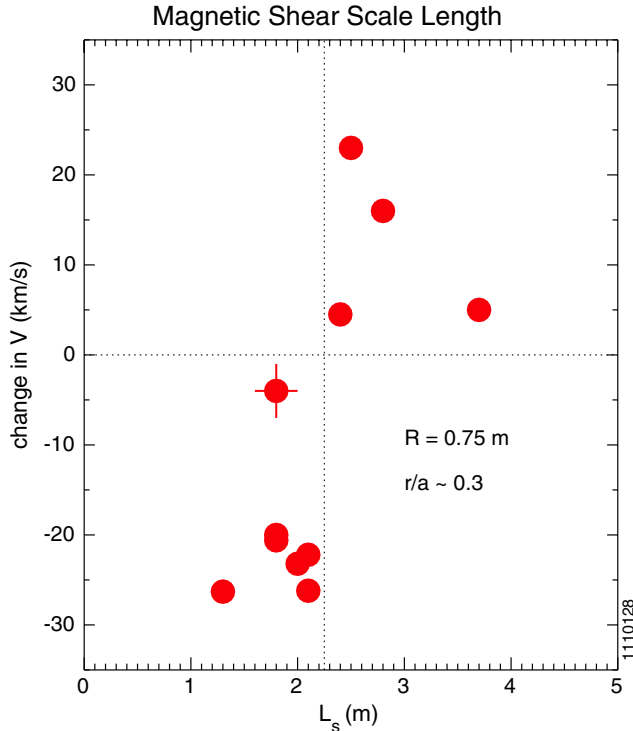

FIG. 5 (color online).   The change in the core rotation velocity with LHCD (1.14–1.24 s) as a function of L_s near $r/a \sim 0.3$ for C-Mod discharges.
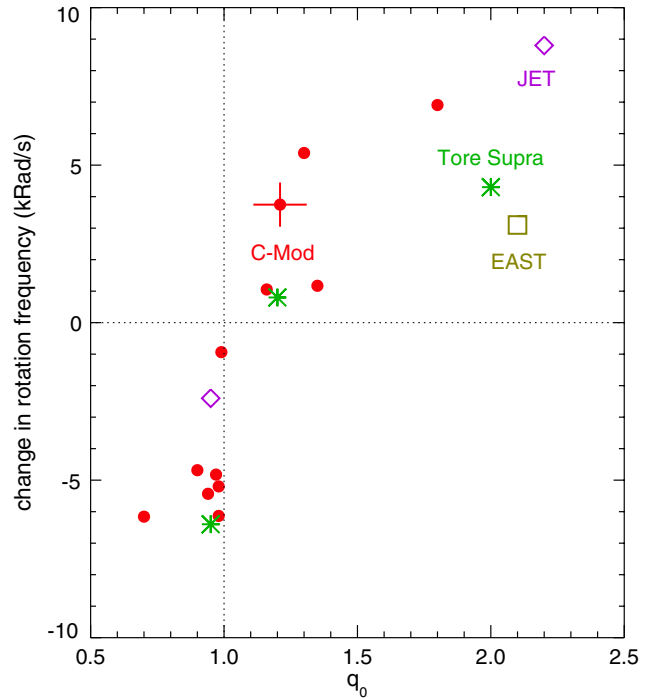

FIG. 6 (color online).   The change in the core rotation frequency with LHCD as a function of q_0. Dots: C-Mod; asterisks: Tore Supra; diamonds: JET; and square: EAST.

acceleration [26] both depend sensitively on the magnetic shear $\hat{s}$ and mode structure via ion-acoustic coupling. In particular, both these drivers of intrinsic rotation require symmetry breaking so as to set a finite value of $\langle k_\perp k_\parallel | \hat{\Phi}_k |^2 \rangle$, necessary for intrinsic torque. Here, the bracket refers to a spectral average. To this end, the intrinsic torque can change noticeably [27] as q' and $\hat{s}$ drop and q'' increases. The effect of q profile modification on the residual stress need not occur via a mode change at all. For example, Ref. [27] shows that a decrease in shear and an increase in q profile curvature may alter the basic symmetry-breaking mechanism for the same basic (ITG) mode. It is evident that a change in symmetry breaking can easily result in a change in sign of the residual stress. Furthermore, the intrinsic torque for the normal magnetic shear and ''flat q'' cases can differ significantly, although this may be an understatement. For weak shear (flat q profiles), nonresonant modes become increasingly important. Recent work [28] has characterized the structure of nonresonant modes and noted that they are best thought of as extended convective cells, with little, if any, similarity to the familiar resonant modes. Further studies [29] have revealed that these nonresonant modes make a substantial contribution to the turbulent heat flux. Thus, there is every reason to expect that the nonresonant modes play an important role in the nondiffusive radial flux of toroidal momentum and the associated Reynolds stress $\langle \tilde{v}_r \tilde{v}_\phi \rangle$. Studies of the effect of nonresonant modes on momentum transport are ongoing and will be discussed in future publications. For now, it should be emphasized that the change in intrinsic torque as LHCD-induced current increases and $q(r)$ flattens is quite likely related to the contributions of nonresonant modes. Previous work on turbulence-driven intrinsic torque has ignored the effect of nonresonant modes.

In summary, LH waves have been introduced into L-mode target plasmas, resulting in velocity changes in both the co- and countercurrent directions. For observations from several tokamaks with LHCD, the rotation direction depends on the resulting changes in the q profile, with corotation increments seen in plasmas with $q_0 > 1$, and countercurrent changes with $q_0 < 1$. This effect likely results from changes in the intrinsic torque (divergence of the residual stress) through changes in the current density profile.

[1] J. E. Rice *et al.*, Nucl. Fusion **47**, 1618 (2007).
[2] Y. Lin, J. Rice, S. Wukitch, M. Greenwald, A. Hubbard, A. Ince-Cushman, L. Lin, M. Porkolab, M. Reinke, and N. Tsujii, Phys. Rev. Lett. **101**, 235002 (2008).
[3] M. Yoshida, Y. Sakamoto, H. Takenaga, S. Ide, N. Oyama, T. Kobayashi, and Y. Kamada, Phys. Rev. Lett. **103**, 065003 (2009).
[4] Y. Sakamoto, S. Ide, M. Yoshida, Y. Koide, T. Fujita, H. Takenaga, and Y. Kamada, Plasma Phys. Controlled Fusion **48**, A63 (2006).
[5] A. Ince-Cushman *et al.*, Phys. Rev. Lett. **102**, 035002 (2009).
[6] J. E. Rice *et al.*, Nucl. Fusion **49**, 025004 (2009).
[7] L.-G. Eriksson, T. Hellsten, M. F. F. Nave, J. Brzozowski, K. Holmström, T. Johnson, J. Ongena, and K.-D. Zastrow, Plasma Phys. Controlled Fusion **51**, 044008 (2009).
[8] Yuejiang Shi *et al.*, Phys. Rev. Lett. **106**, 235001 (2011).
[9] J. E. Rice *et al.*, Nucl. Fusion **53**, 093015 (2013).
[10] M. F. F. Nave *et al.*, "Scalings of Spontaneous Rotation in the JET Tokamak" (unpublished).
[11] Z. Gao, N. J. Fisch, and H. Qin, Phys. Plasmas **18**, 082507 (2011).
[12] J. Lee, F. I. Parra, R. R. Parker, and P. T. Bonoli, Plasma Phys. Controlled Fusion **54**, 125005 (2012).
[13] Xiaoyin Guan, H. Qin, J. Liu, and N. J. Fisch, Phys. Plasmas **20**, 022502 (2013).
[14] A. Ince-Cushman *et al.*, Rev. Sci. Instrum. **79**, 10E302 (2008).
[15] J. E. Rice *et al.*, Nucl. Fusion **51**, 083005 (2011).
[16] J. E. Rice *et al.*, Phys. Rev. Lett. **107**, 265001 (2011).
[17] J. E. Rice *et al.*, Phys. Plasmas **19**, 056106 (2012).
[18] A. Bortolon, B. P. Duval, A. Pochelon, and A. Scarabosio, Phys. Rev. Lett. **97**, 235003 (2006).
[19] P. H. Diamond, C. J. McDevitt, Ö. D. Gürcan, T. S. Hahm, W. X. Wang, E. S. Yoon, I. Holod, Z. Lin, V. Naulin, and R. Singh, Nucl. Fusion **49**, 045002 (2009).
[20] Ö. D. Gürcan, P. H. Diamond, T. S. Hahm, and R. Singh, Phys. Plasmas **14**, 042306 (2007).
[21] Y. Kosuga, P. H. Diamond, and O. D. Gurcan, Phys. Plasmas **17**, 102313 (2010).
[22] Ö. D. Gürcan, P. H. Diamond, P. Hennequin, C. J. McDevitt, X. Garbet, and C. Bourdelle, Phys. Plasmas **17**, 112309 (2010).
[23] J. E. Rice *et al.*, Phys. Rev. Lett. **106**, 215001 (2011).
[24] J. Ko, S. Scott, S. Shiraiwa, M. Greenwald, R. Parker, and G. Wallace, Rev. Sci. Instrum. **81**, 033505 (2010).
[25] S. Shiraiwa *et al.*, Phys. Plasmas **18**, 080705 (2011).
[26] L. Wang and P. H. Diamond, "Gyrokinetic Theory of Turbulent Acceleration of Parallel Rotation in Tokamak Plasmas" (unpublished).
[27] J. M. Kwon, S. Yi, T. Rhee, P. H. Diamond, K. Miki, T. S. Hahm, J. Y. Kim, Ö. D. Gürcan, and C. McDevitt, Nucl. Fusion **52**, 013004 (2012).
[28] S. Yi, J. M. Kwon, P. H. Diamond, and T. Rhee, Phys. Plasmas **19**, 112506 (2012).
[29] S. Yi *et al.* (unpublished).
[30] F. Romanelli *et al.*, *Proceedings of the 24th IAEA Fusion Energy Conference, San Diego, 2012* [International Atomic Energy Agency (IAEA), Trieste, 2012]. (All members of the JET-EFDA Collaboration appear in the appendix of this paper.)